potential of the As_2Mo_2 rhombus.

Acknowledgment. The authors are grateful to R. Hoffmann for a helpful discussion about the isolobal relationships. Support for this work was obtained, in part, from the University of Delaware Center for Catalytic Science and Technology and from the donors of the Petroleum Research Fund, administered by the American Chemical Society.

Supplementary Material Available: Complete listings of bond distances and angles, anisotropic temperature coefficients, and hydrogen atom coordinates for **1**, **2**, and **3** (13 pages); listing of observed and calculated structure factors for **1–3** (56 pages). Ordering information is given on any current masthead page.

Synthesis, Characterization, and Reactivity of α-Ketoacyl Complexes of Platinum(II) and Palladium(II). Crystal Structures of *trans*-$Pt(PPh_3)_2(Cl)(COCOPh)$ and *cis*-$Pt(PPh_3)_2(COPh)(COOMe)$

Ayusman Sen,*[1] Jwu-Ting Chen,[2a] William M. Vetter, and Robert R. Whittle[2b]

Contribution from the Chandlee Laboratory, Department of Chemistry, Pennsylvania State University, University Park, Pennsylvania 16802. *Received May 14, 1986*

Abstract: The α-ketoacyl chloro complexes, *trans*-$M(PPh_3)_2(Cl)(COCOR)$ (M = Pt: R = Ph, **1a**; R = *p*-FC_6H_4, **1b**; R = *p*-ClC_6H_4, **1c**; R = *p*-MeC_6H_4, **1d**; R = Me, **1e**. M = Pd: R = Ph, **2**), were synthesized by the oxidative addition of the appropriate α-ketoacyl chloride with either $Pt(PPh_3)_4$ or $Pd(PPh_3)_4$. The crystal structure of **1a** showed a square-planar geometry around the Pt with the two carbonyl groups virtually coplanar and in an s-trans configuration. The above compounds were found to decompose thermally to the corresponding benzoyl compounds, *trans*-$M(PPh_3)_2(Cl)(COR)$. A detailed kinetic study of the decarbonylation of **1a** and **2** indicated the presence of two competing pathways, one of which involved the initial dissociation of a PPh_3 ligand. The kinetic and thermodynamic parameters for the various steps in the mechanism were determined. For the decarbonylation of compounds **1a–d**, a correlation was observed between the rate constant for the phosphine-independent pathway and σ_{para}. The cationic α-ketoacyl complexes, *trans*-$Pt(PPh_3)_2(L)(COCOR)^+BF_4^-$ (R = Ph: L = CH_3CN, **4a**; L = CO, **4b**; L = PPh_3, **4c**. R = Me: L = CH_3CN, **4d**), were prepared by Cl^- abstraction from the corresponding neutral compounds in the presence of an appropriate ligand. In the absence of any added ligand, the Cl^- abstraction from **1a** resulted in rapid deinsertion of CO to form *cis*-$Pt(PPh_3)_2(CO)(COPh)^+$ (**5a**) initially, which then slowly converted to the corresponding trans compound, **5b**. The decarbonylation of **1a** to the corresponding chloro benzoyl compound was catalyzed by the addition of **5b**. The addition of OMe^- to **5a** and **5b** resulted in the formation of the acyl–alkoxycarbonyl complexes *cis*- and *trans*-$Pt(PPh_3)_2(COPh)(COOMe)$, **6a** and **6b**, respectively. Similarly, *trans*-$Pt(PPh_3)_2(COCOPh)(COOMe)$ (**6d**) was formed by the reaction of OMe^- with **4b**. The crystal structure of **6a** revealed a square-planar geometry around the Pt with the COPh and COOMe groups lying in planes perpendicular to the plane of the molecule.

The 1,2-shift of alkyl and aryl groups between a metal center and the carbon atom of a coordinated CO molecule (eq 1) is frequently observed and is a well-studied reaction.[3] In contrast, the corresponding migration of an acyl group from the metal to the CO ligand (eq 2) has never been observed. The reverse

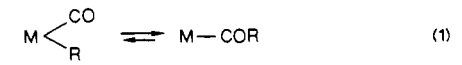

(1)

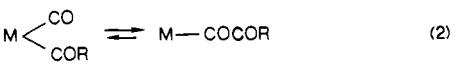

(2)

reaction, although known,[4,5] remains poorly defined from a mechanistic standpoint, mainly due to the paucity of well-characterized α-ketoacyl compounds.[4-6] Herein, we describe the synthesis and characterization of a family of neutral and cationic Pt(II) and Pd(II) α-ketoacyl compounds. We also report the results of our studies on the mechanism of acyl migration from a coordinated CO to the metal center. Our studies have allowed

Scheme I

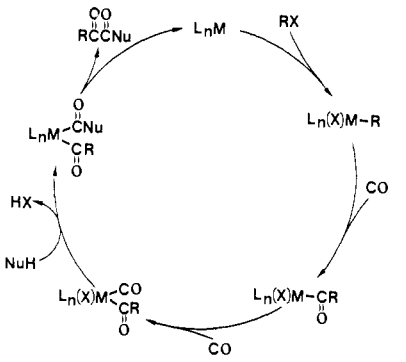

(1) Alfred P. Sloan Research Fellow, 1984–1986.
(2) (a) Current address: Department of Chemistry, National Taiwan University, Taipei, Taiwan, ROC. (b) X-ray crystallography.
(3) (a) Kochi, J. K. *Organometallic Mechanisms and Catalysis*; Academic: New York, 1978; Chapter 18. (b) Collman, J. P.; Hegedus, L. S. *Principles and Applications of Organotransition Metal Chemistry*; University Science Books: Mill Valley, CA, 1980; Chapter 5. (c) For reactions involving group 10 metals in particular, see: Anderson, G. K.; Cross, R. J. *Acc. Chem. Res.* **1984**, *17*, 67.
(4) (a) Casey, C. P.; Bunnell, C. A.; Calabrese, J. C. *J. Am. Chem. Soc.* **1976**, *98*, 1166. (b) Ozawa, F.; Sugimoto, T.; Yamamoto, T.; Yamamoto, A. *Organometallics* **1984**, *3*, 692.
(5) Chen, J.-T.; Sen, A. *J. Am. Chem. Soc.* **1984**, *106*, 1506.
(6) (a) Blake, D. M.; Vinson, A.; Dye, R. *J. Organomet. Chem.* **1981**, *204*, 257. (b) Selover, J. C.; Vaughn, G. D.; Strouse, C. E.; Gladysz, J. A. *J. Am. Chem. Soc.* **1986**, *108*, 1455. (c) For the synthesis of alkoxalyl complexes, see: Dobrzynski, E. D.; Angelici, R. J. *Inorg. Chem.* **1975**, *14*, 59. Fayos, J.; Dobrzynski, E.; Angelici, R. J.; Clardy, J. *J. Organomet. Chem.* **1973**, *59*, C33.

0002-7863/87/1509-0148$01.50/0 © 1987 American Chemical Society

Table I. ^{31}P NMR ($CDCl_3$) and IR (KBr) Data for the Complexes

complex	δ^a (J_{Pt-P}, Hz)	$\bar{\nu}$(CO), cm^{-1}
trans-$Pt(PPh_3)_2(Cl)(COCOPh)$, **1a**	16.54 (3286.9)	1660, 1640
trans-$Pt(PPh_3)_2(Cl)(COCOC_6H_4F\text{-}p)$, **1b**	16.49 (3268.8)	1660, 1636
trans-$Pt(PPh_3)_2(Cl)(COCOC_6H_4Cl\text{-}p)$, **1c**	16.43 (3259.3)	1662, 1638
trans-$Pt(PPh_3)_2(Cl)(COCOC_6H_4Me\text{-}p)$, **1d**	16.67 (3296.0)	1657, 1637
trans-$Pt(PPh_3)_2(Cl)(COCOMe)$, **1e**	16.25 (3263.2)	1694, 1634
trans-$Pd(PPh_3)_2(Cl)(COCOPh)$, **2**	16.50	1680, 1650
trans-$Pt(PPh_3)_2(Cl)(COPh)$, **3a**	17.89 (3382.9)	1613
trans-$Pd(PPh_3)_2(Cl)(COPh)$, **3b**	16.69	1635
trans-$Pt(PPh_3)_2(CH_3CN)(COCOPh)^+$, **4a**	18.31 (3199.1)	1670, 1655
trans-$Pt(PPh_3)_2(CO)(COCOPh)^+$, **4b**	11.43 (2815.0)	
trans-$Pt(PPh_3)_3(COCOPh)^+$, **4c**	11.04 (d, 3048.5) 10.00 (t, 1680.9) (J_{P-P} = 26.1)	
trans-$Pt(PPh_3)_2(CH_3CN)(COCOMe)^+$, **4d**	18.70 (3182.5)	1698, 1642
cis-$Pt(PPh_3)_2(CO)(COPh)^+$, **5a**	11.91 (d, 3795.0) 7.54 (d, 1493.5) (J_{P-P} = 29.5)	
trans-$Pt(PPh_3)_2(CO)(COPh)^+$, **5b**	11.79 (2950.5)	2070, 1630
cis-$Pt(PPh_3)_2(COPh)(COOMe)$, **6a**	14.55 (d, 2205.8) 7.69 (d, 1502.6) (J_{P-P} = 20.3)	1632, 1615
trans-$Pt(PPh_3)_2(COPh)(COOMe)$, **6b**	14.47 (3229.3)	1625, 1602
trans-$Pt(PPh_3)_2(COPh)(COOEt)$, **6c**	14.53 (3193.7)	1620, 1601
trans-$Pt(PPh_3)_2(COCOPh)(COOMe)$, **6d**	13.59 (3193.1)	1662, 1632, 1628

[a] In ppm.

us to construct a reaction coordinate profile in one case, and in addition, we now have the rare opportunity to directly compare the energetics of the migratory deinsertion step both for a given metal in two different coordination geometries (four-coordinate Pd(II) vs. three-coordinate Pd(II)) and for two different metals from the same group in identical coordination geometries (four-coordinate Pd(II) vs. four-coordinate Pt(II)). It has also been possible to correlate the migration rate with the electron-releasing ability of the acyl group.

Our studies on the decomposition of cationic α-ketoacyl compounds of Pt(II) also led to the synthesis and characterization of both cis and trans acyl–alkoxycarbonyl complexes of Pt(II). These constitute, with one exception,[7] the first examples of species of the type RCO–M–CONu, which are the proposed key intermediates in the catalytic "double carbonylation" of alkyl and aryl halides (Scheme I),[5,8] a reaction of considerable practical importance.[9] We have also synthesized an α-ketoacyl–alkoxycarbonyl complex of Pt(II), *trans*-$Pt(PPh_3)_2(COCOPh)(COOMe)$.

Results and Discussion

A. Synthesis and Characterization of the α-Ketoacyl Chloro Complexes. The α-ketoacyl chloro complexes, **1a–e** and **2**, were prepared by the oxidative addition of the appropriate α-ketoacyl chloride to either $Pt(PPh_3)_4$ or $Pd(PPh_3)_4$ in benzene (eq 3). In the synthesis of **2**, an excess of PPh_3 was added to the reaction mixture to retard the decomposition of the product (see section B).

$$M(PPh_3)_4 + RCOCOCl \xrightarrow{\text{benzene}} \textit{trans}\text{-}M(PPh_3)_2(Cl)(COCOR) \quad (3)$$

M = Pt: R = Ph, **1a**; R = *p*-FC_6H_4, **1b**; R= *p*-ClC_6H_4, **1c**; R = *p*-MeC_6H_4, **1d**; R = Me, **1e**; M = Pd: R = Ph, **2**

All of the aryloylformyl complexes were red-orange solids, while the pyruvoyl complex was yellow-orange. The compounds were soluble in dichloromethane, chloroform, and benzene but insoluble in ethers and alkanes. The Pd(II) complex, **2**, slowly decomposed in solution at 25 °C to the corresponding benzoyl complex, while the Pt(II) compounds were stable indefinitely in solution at 25 °C (see section B).

The spectral data for the compounds are presented in Table I. The ^{31}P NMR spectra consisted of singlets, accompanied by ^{195}Pt satellites in the case of the Pt(II) compounds, and were consistent with square-planar structures containing two equivalent *trans*-phosphine ligands. For the Pt(II) compounds, **1a–d**, the ^{195}Pt–^{31}P coupling constant was found to increase with increasing electron-donating ability of the para substituent. Indeed, a good correlation of this parameter with the Hammett σ_{para} parameter was observed (Figure 1).

All the compounds showed two $\bar{\nu}$(CO) bands attributable to the α-ketoacyl ligand in their IR spectra. The higher frequency

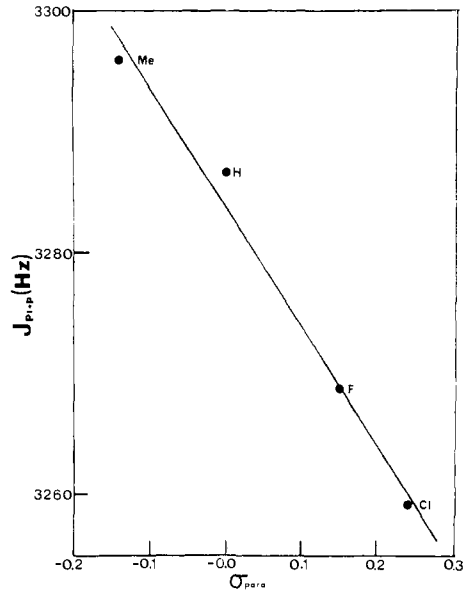

Figure 1. Hammett plot for the effect of the para substituent on the ^{195}Pt–^{31}P coupling constant for Pt(II)–benzoylformyl complexes, **1a–d**.

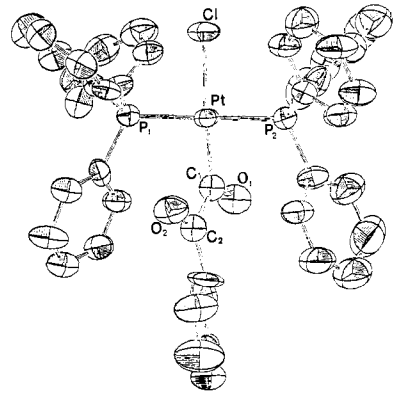

Figure 2. ORTEP drawing of *trans*-$Pt(PPh_3)_2(Cl)(COCOPh)$.

(7) For the synthesis of $Pt(dppe)(COC_6H_9)(COOH)$, see: Bennett, M. A.; Rokicki, A. *Organometallics* **1985**, *4*, 180.

(8) (a) Ozawa, F.; Sugimoto, T.; Yuasa, Y.; Santra, M.; Yamamoto, T.; Yamamoto, A. *Organometallics* **1984**, *3*, 683. (b) Reference 4b. (c) Ozawa, F.; Soyama, H.; Yanagihara, H.; Aoyama, I.; Takino, H.; Izawa, K.; Yamamoto, Y.; Yamamoto, A. *J. Am. Chem. Soc.* **1985**, *107*, 3235.

(9) (a) Ozawa, F.; Soyama, H.; Yamamoto, T. *Tetrahedron Lett.* **1982**, *23*, 3383. (b) Ozawa, F.; Kawasaki, N.; Yamamoto, T.; Yamamoto, A. *Chem. Lett.* **1985**, 567. (c) Reference 8c. (d) Kobayashi, T.; Tanaka, M. *J. Organomet. Chem.* **1982**, *233*, C64. (e) Tanaka, M.; Kobayashi, T.; Sakakura, T. *J. Chem. Soc., Chem. Commun.* **1985**, 837. (f) Alper, H.; Des Abbayes, H. *J. Organomet. Chem.* **1977**, *134*, C11. (g) Des Abbayes, H.; Bulop, A. *J. Chem. Soc., Chem. Commun.* **1978**, 1090. (h) Alper, H.; Arzoumanian, H.; Petrignani, J. F.; Saldana, M. M. *J. Chem. Soc., Chem. Commun.* **1985**, 340. (i) Cassar, L.; Foa, M. *J. Organomet. Chem.* **1977**, *134*, C15. (j) Francalanci, F.; Foa, M. *J. Electroanal. Chem.* **1982**, *232*, 59. (k) Foa, M.; Moro, A.; Gardano, A.; Cassar, L. *U.S. Patent* 4351952, 1982. (l) Fell, B.; Chrobaczek, H. *Chem.-Ztg.* **1984**, *108*, 291. (m) Lee, J. Y.; Walter, T. J. *U.S. Patent* 4473706, 1984. (n) Wolfram, J. W. *U.S. Patent* 4481368, 1984. (o) Wolfram, J. W. *U.S. Patent* 4481369, 1984. (p) Lee, J. Y.; Wolfram, J. W. *U.S. Patent* 4492798, 1986.

Table II. Selected Bond Distances (Å) and Angles (Deg) for *trans*-Pt(PPh_3)$_2$(Cl(COCOPh)[a]

atom 1	atom 2	distance
Pt	Cl	2.421 (3)
Pt	P1	2.306 (3)
Pt	P2	2.307 (3)
Pt	C1	2.018 (1)
Pt	C1A	2.047 (1)
O1	C1	1.303 (9)
O1	C2A	1.367 (9)
O2	C1A	1.230 (8)
O2	C2	1.189 (8)
C1	C1A	1.107 (1)
C1	C2	1.560 (1)
C1A	C2A	1.667 (1)
C2	C2A	1.253 (1)
C2	C3	1.75 (3)
C2A	C3	1.511 (14)

atom 1	atom 2	atom 3	angle
Cl	Pt	P1	91.0 (1)
Cl	Pt	P2	87.9 (1)
Cl	Pt	C1	173.0 (1)
Cl	Pt	C1A	155.3 (1)
P1	Pt	P2	178.9 (1)
P1	Pt	C1	89.12 (9)
P1	Pt	C1A	94.27 (9)
P2	Pt	C1	94.94 (9)
P2	Pt	C1A	86.71 (8)
C1	Pt	C1A	31.61 (1)
O2	C2	C1	109.4 (4)
O2	C2	C2A	154.8 (4)
O2	C2	C3	148.0 (1)
C1	C2	C3	101.4 (9)
O1	C2A	C1A	103.1 (4)
O1	C2A	C3	131.0 (1)
Pt	C1	O1	119.9 (4)
Pt	C1	C2	120.40 (1)
O1	C1	C2	119.3 (4)
Pt	C1A	O2	135.7 (4)
Pt	C1A	C2A	114.50 (1)
O2	C1A	C2A	109.8 (4)
C1A	C2A	C3	119.0 (1)
C2	C3	C2A	44.5 (7)

[a] Numbers in parentheses are estimated standard deviations in the least significant digits.

absorption was not significantly different from that observed for the corresponding α-keto acid and was assigned to the β-carbonyl group. The lower frequency band at ca. 1640 cm^{-1} was substantially lower than the α-carbonyl band in the corresponding acid (ca. 1725 cm^{-1}) and was presumably due to the replacement of an electron-withdrawing OH group by an electron-releasing metal fragment. We note that our assignment of the two $\bar{\nu}$(CO) absorptions is also consistent with that observed in related compounds.[4-6] However, unlike several of these compounds which[4,6c] show two sets of $\bar{\nu}$(CO) bands due to the presence of s-trans and s-cis rotamers, either in solution or in the solid state, only one rotamer (presumably s-trans, see Figure 2) appears to be present in our compounds, at least in the solid state.

The ^{13}C NMR spectrum of **1e** exhibited resonances at 214.4 and 200.5 ppm due to the carbonyl carbons of the α-ketoacyl ligand. The higher field resonance showed significantly larger $^{195}Pt-^{13}C$ coupling (195 vs. 14 Hz) and was assigned to the α-carbonyl group.

The solid-state structure of **1a** was confirmed by X-ray crystallography and is shown in Figure 2. The four ligands were found to be disposed about the central Pt atom in a square-planar geometry with the two phosphines in mutually trans positions. The Pt-P distances (2.306 (3) and 2.307 (3) Å) and the Pt-Cl distance (2.421 (3) Å) were normal (Table II). The two carbonyl groups of the benzoylformyl ligand were virtually coplanar (dihedral angle of 3.3°) and in an s-trans configuration as seen also in previously reported analogues.[4a,6c] On the other hand, the phenyl group was twisted out of the plane of the β-carbonyl group by 25.7°. A positional disorder existed for the two carbonyl carbon atoms

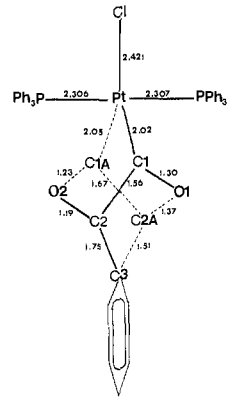

Figure 3. Positional disorder of the carbonyl groups in *trans*-Pt(PPh_3)$_2$(Cl)(COCOPh).

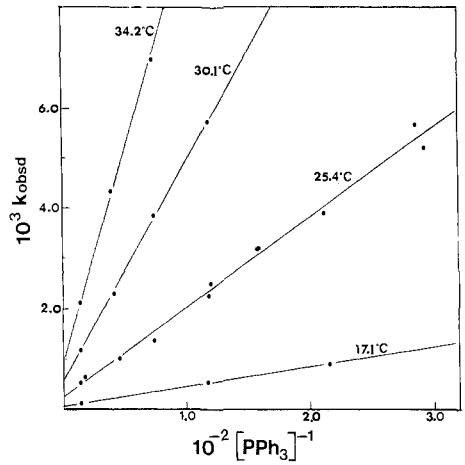

Figure 4. Plots of k_{obsd} vs. $[PPh_3]^{-1}$ for the decarbonylation of *trans*-Pd(PPh_3)$_2$(Cl)(COCOPh) in CH_2Cl_2.

because of a 180° rotation about the twofold axis through the Pt-Cl bond (Figure 3). In the final least-squares cycle, all non-hydrogen atoms except the two disordered carbon atoms were refined anisotropically, no attempt being made to refine the positional disorder. Therefore, the structural parameters for the carbonyl groups deviate from normal values.

B. Thermal Decarbonylation of the α-Ketoacyl Chloro Complexes. The compounds **1a-e** and **2** were found to decarbonylate thermally in solution to the corresponding acyl complexes (eq 4).

$$trans\text{-}M(PPh_3)_2(Cl)(COCOR) \xrightarrow[\Delta]{solv} trans\text{-}M(PPh_3)_2(Cl)(COR) + CO \quad (4)$$

For the Pd(II) compound, **2**, the decarbonylation rate was appreciable at 25 °C, whereas the Pt(II) compounds underwent decarbonylation at a significant rate only at significantly higher temperatures (>60 °C). This reaction could be monitored by ^{31}P NMR, by IR, and most conveniently, by visible spectroscopies. All the α-ketoacyl chloro complexes exhibited a strong absorption band at 450-500 nm, which disappeared on decarbonylation to the corresponding acyl compounds.

In the presence of excess added PPh_3, the decarbonylation rates of the compounds **1a-e** and **2** were found to obey the following empirical rate equation

$$-d[M\text{-}COCOR]/dt = (a + b/[PPh_3])[M\text{-}COCOR] \quad (5)$$

Equation 5 is compatible with the following formal rate expression

$$-d[M\text{-}COCOR]/dt = (k_1 + k_2K/[PPh_3])[M\text{-}COCOR] = k_{obsd}[M\text{-}COCOR] \quad (6)$$

which may be derived from the mechanism of eq 7 by assuming $K \ll [PPh_3]$. A plot of k_{obsd} vs. $[PPh_3]^{-1}$ would allow the determination of k_1 and k_2K from the intercept and the slope, re-

Table III. Kinetic Parameters for the Decarbonylation of α-Ketoacyl Chloro Complexes[a]

complex	temp, °C	k_1, s^{-1}	k_2K, M s^{-1}	k_2, s^{-1}	K, M
1a[b]	70.0	2.63 (10) × 10^{-5}			
	80.0	8.36 (30) × 10^{-5}			
	90.0	2.98 (10) × 10^{-4}			
1b[b]	80.0	6.09 (10) × 10^{-5}			
1c,[b]	80.0	5.65 (20) × 10^{-5}			
1d,[b]	80.0	1.20 (10) × 10^{-4}			
2[c]	17.1	7.96 (1.60) × 10^{-5}	3.93 (11) × 10^{-6}	0.148 (26)	2.65 (47) × 10^{-5}
	25.4	2.68 (98) × 10^{-4}	1.78 (6) × 10^{-5}	0.389 (52)	4.58 (59) × 10^{-5}
	30.1	5.76 (56) × 10^{-4}	4.34 (8) × 10^{-5}	0.599 (59)	7.25 (70) × 10^{-5}
	34.2	9.60 (1.47) × 10^{-4}	8.17 (30) × 10^{-5}	0.906 (93)	9.02 (86) × 10^{-5}

[a] Numbers in parentheses are estimated standard deviations. [b] In toluene, $[PPh_3]_{add}$ = 8.99 × 10^{-2} M. [c] In CH_2Cl_2.

spectively. For the Pd(II) compound, **2**, the plots obtained at four different temperatures in CH_2Cl_2 are shown in Figure 4.

$$M(PPh_3)_2(Cl)(COCOR) \xrightarrow{k_1} M(PPh_3)_2(Cl)(CO)(COR)$$

$$M(PPh_3)_2(Cl)(CO)(COR) \xrightarrow{\text{fast}} M(PPh_3)_2(Cl)(COR) + CO$$

$$M(PPh_3)_2(Cl)(COCOR) \overset{K}{\rightleftharpoons} M(PPh_3)(Cl)(COCOR) + PPh_3$$

$$M(PPh_3)(Cl)(COCOR) \xrightarrow{k_2} M(PPh_3)(Cl)(CO)(COR)$$

$$M(PPh_3)(Cl)(CO)(COR) \xrightarrow[\text{fast}]{PPh_3} M(PPh_3)_2(Cl)(COR) + CO \quad (7)$$

In the absence of any added Ph_3P, the thermal decarbonylation of **2** also followed pseudo-first-order kinetics. This was understandable if one made the reasonable assumption that the equilibrium constants for the phosphine dissociation step were similar for **2** and its decomposition product, *trans*-$Pd(PPh_3)_2(Cl)(COPh)$ (**3b**), so that the concentration of free PPh_3 remained essentially unchanged throughout the course of the reaction. This then allowed us the opportunity to determine the values of K and k_2 separately in the following way.

The concentration of free PPh_3, $[PPh_3]_0$, in the runs carried out in the absence of added PPh_3 could be evaluated by plugging the measured k_{obsd} values into the plots of Figure 4. In the absence of added PPh_3, the equilibrium constant K for the PPh_3 dissociation step is approximated by eq 8

$$K = \frac{[Pd(PPh_3)(Cl)(COCOPh)]\,[PPh_3]_0}{[Pd(PPh_3)_2(Cl)(COCOPh)]} = \frac{[PPh_3]_0^2}{[Pd]_0 - [PPh_3]_0} \quad (8)$$

where $[Pd]_0$ is the initial concentration of **2**. In general

$$K = \frac{[Pd(PPh_3)(Cl)(COCOPh)][PPh_3]_{tot}}{[Pd(PPh_3)_2(Cl)(COCOPh)]} \quad (9)$$

where $[PPh_3]_{tot}$ is the sum of the concentrations of dissociated PPh_3, $[PPh_3]_{dissoc}$, and added PPh_3, $[PPh_3]_{add}$. With the values of K obtained through eq 8 and the known values of $[Pd]_0$ and $[PPh_3]_{add}$, $[PPh_3]_{dissoc}$ values for individual runs were determined using eq 10. With the corrected $[PPh_3]_{tot}$, new plots of k_{obsd} vs.

$$K = \frac{[PPh_3]_{dissoc}([PPh_3]_{dissoc} + [PPh_3]_{add})}{([Pd]_0 - [PPh_3]_{dissoc})} \quad (10)$$

$[PPh_3]^{-1}$ were constructed, and $[PPh_3]_0$ and K were reevaluated from these. This procedure was repeated until the values of $[PPh_3]_0$, $[PPh_3]_{tot}$, and K converged. The final values of k_1, k_2K, k_2, and K are given in Table III. The numbers support our assumption, $K \ll [PPh_3]$, which was used to derive eq 6, valid for the runs carried out with excess added PPh_3. Figure 5 illustrates the Eyring relationships for k_1, k_2K, k_2, and K. From these the activation parameters ($\Delta H^\ddagger$, $\Delta S^\ddagger$ for k_1, k_2K, k_2; $\Delta H°$, $\Delta S°$, $\Delta G°$ for K) were determined and are listed in Table IV.

The rate of decarbonylation of **2** was unaffected at 25 °C by the presence of CO up to a pressure of 700 psi. Similarly, no trace of **2** was observed when the corresponding benzoyl compound **3b** was exposed to 1000 psi of CO at 25 °C. With an initial concentration of 0.05 M for **3b** and a detection limit of 0.01 AU at 494 nm (ϵ_{max} 80 M^{-1} cm^{-1}), corresponding to a concentration of 1.25 × 10^{-4} M for **2**, K_{eq} (for **2** ⇌ **3b** + CO) was calculated to be >220 M at 25 °C. Hence $\Delta G°$ for the overall decarbonylation reaction was <−3.2 kcal mol^{-1}. Using this value, and the $\Delta G^\ddagger$ and $\Delta G°$ values from Table IV, we constructed the reaction coordinate profile shown in Figure 6.

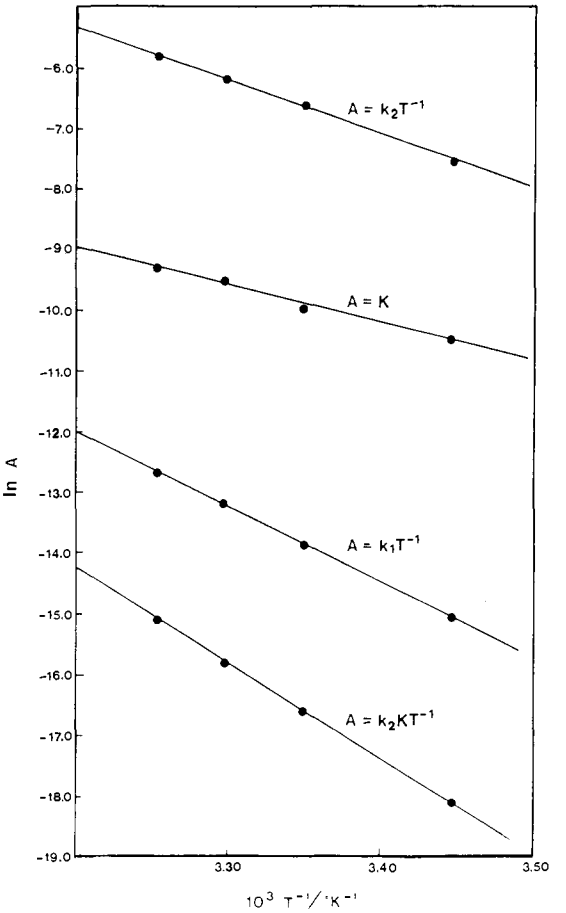

Figure 5. Eyring plots for the decarbonylation of *trans*-$Pd(PPh_3)_2(Cl)(COCOPh)$.

Table IV. Thermodynamic Parameters for the Decarbonylation of α-Ketoacyl Chloro Complexes[a]

complex	kinetic parameter	$\Delta H^\ddagger$, $\Delta H°$ (kcal mol^{-1})	$\Delta S^\ddagger$, $\Delta S°$ (cal mol^{-1} K^{-1})	$\Delta G^\ddagger$, $\Delta G°$[b] (kcal mol^{-1})
1a	k_1	29.2 (6)	5.4 (4.4)	27.3 (1)
2	k_1	25.4 (6)	10.4 (2.0)	22.3 (1)
	k_2K	31.1 (9)	23.9 (3.1)	23.9 (1)
	k_2	18.1 (5)	0.1 (1.7)	18.1 (1)
	K[b]	13.0 (7)	23.9 (2.3)	5.9 (1)

[a] Numbers in parentheses are estimated standard deviations. [b] At 25 °C.

Like the Pd(II) compound, **2**, the decarbonylation of the Pt(II) compounds, **1a–e**, also followed a pseudo-first-order rate law with

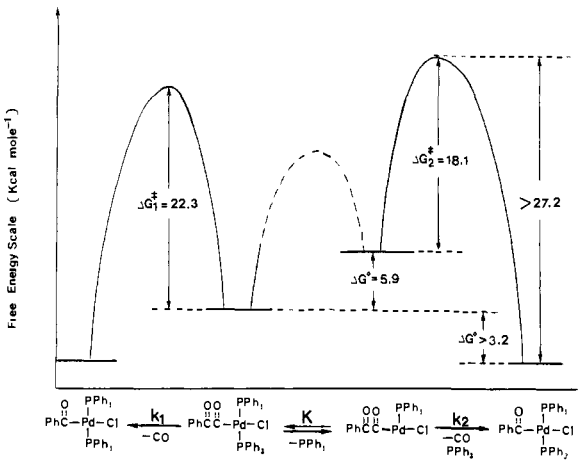

Figure 6. Free energy profile for the decarbonylation of *trans*-Pd(PPh$_3$)$_2$(Cl)(COCOPh).

the rate decreasing to a limiting value with increasing concentration of added PPh$_3$. For compounds **1a–d**, a PPh$_3$ concentration of 8.99×10^{-2} M was found to be sufficient to suppress the phosphine-dependent pathway so that the observed rate constant was equal to the first-order rate constant, k_1, of eq 7. An analysis of the tempeature dependence of k_1 for compound **1a** in toluene (Table III) yielded the activation parameters listed in Table IV.

Table IV and Figure 6 contain several interesting features. A number of reactions of compounds of the type M(PR$_3$)$_2$(X)(Y) have been investigated, and with few exceptions, they involve the initial dissociation of a phosphine ligand.[10] Surprisingly, however, there does not appear to be any previous data on this dissociation step. The moderately positive $\Delta S°$ value is consistent with a dissociative process, and the $\Delta H°$ value of 13 kcal mol^{-1} must reflect in large part the Pd–PPh$_3$ bond dissociation energy. More importantly, we now have the rare opportunity to compare the energetics of the deinsertion step both for a given metal in two different coordination geometries (four-coordinate Pd(II) vs. three-coordinate Pd(II)) and for two different metals from the same group in identical coordination geometries (four-coordinate Pd(II) vs. four-coordinate Pt(II)). The $\Delta H^‡$ associated with the migratory deinsertion step appears to vary substantially with both the coordination geometry and the metal involved. The migration may be viewed as a nucleophilic or an anionotropic 1,2-shift, with a transition state illustrated below. An electron-deficient mi-

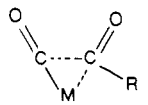

gration terminus would clearly favor such a shift, and hence, $\Delta H^‡$ associated with the three-coordinate 14-electron Pd(II) center is significantly lower than that associated with the corresponding four-coordinate 16-electron metal center. The greater $\Delta H^‡$ for migration in the four-coordinate Pt(II) center compared to that

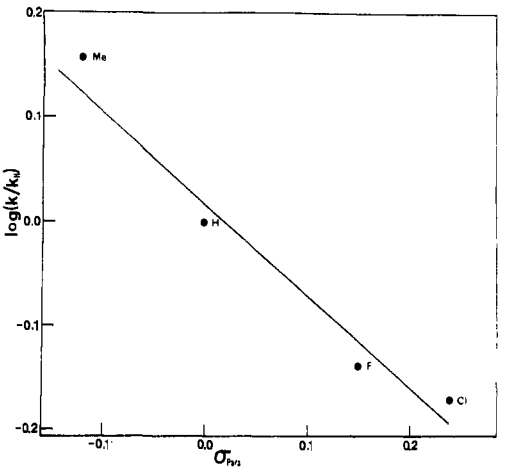

Figure 7. Hammett plot for the effect of the para substituent on the phosphine-independent pathway (k_1) for the decarbonylation of Pt(II)–benzoylformyl complexes, **1a–d**.

for the corresponding Pd(II) center is less easily understood. The electron affinity[11] and metal–ligand bond energies[12] are higher for Pt(II) than for Pd(II). Thus, one would have expected a higher migration rate for the Pt(II) system, especially since the PhCO–COM bond energy would not be expected to vary significantly with the metal. The $\Delta S^‡$ values, in contrast, were similar and within the range observed for CO insertion reactions such as eq 11.[13]

$$Pt(PR_3)_2(I)(CO)(Ar) \rightarrow Pt(PR_3)_2(I)(COAr) \quad (11)$$

A Hammett plot of the rate constant for the phosphine-independent pathway, k_1, for **1a–d** vs. σ_{para} is shown in Figure 7. For this plot, $\rho = -0.88$ was obtained. A similar plot vs σ_{para}^+ showed a significantly weaker correlation. These results indicated that electron-donating substituents on the β-carbonyl group accelerated the deinsertion process[14] and, furthermore, that the direct resonance interaction of the aryl group with the β-carbonyl group in the transition state was minimal. The latter was perhaps due to the twisting of the aryl ring to reduce unfavorable steric interactions. Indeed, as the structure of **1a** indicated, even in the ground state the phenyl group was twisted away from the plane of the β-carbonyl group by 25.7°.

C. Synthesis and Reactivity of the Cationic α-Ketoacyl Complexes. The treatment of **1a** and **1e** with equimolar amounts of AgBF$_4$ in CH$_3$CN solution resulted in the formation of the corresponding cationic complexes, *trans*-Pt(PPh$_3$)$_2$(CH$_3$CN)(COCOR)$^+$BF$_4^-$ (R = Ph, **4a**; R = Me, **4d**). Both these compounds were stable as solids and in solution at 25 °C. Like their parent compounds, **1a** and **1e**, their ^{31}P NMR spectra consisted of singlets accompanied by ^{195}Pt satellites, and they exhibited two $\bar{\nu}$(CO) bands attributable to the α-ketoacyl ligand in their IR spectra.

In analogous reactions, the abstraction of Cl$^-$ from **1a** by AgBF$_4$ in CH$_2$Cl$_2$ in the presence of CO and PPh$_3$ caused the formation of *trans*-Pt(PPh$_3$)$_2$(CO)(COCOPh)$^+$BF$_4^-$ (**4b**) and *trans*-Pt(PPh$_3$)$_3$(COCOPh)$^+$BF$_4^-$ (**4c**), respectively. These reactions are summarized in eq 12.

$$trans\text{-}Pt(PPh_3)_2(Cl)(COCOR) \xrightarrow[L]{AgBF_4} trans\text{-}Pt(PPh_3)_2(L)(COCOR)^+BF_4^- \quad (12)$$

R = Ph: L = CH$_3$CN, **4a**; L = CO, **4b**; L = PPh$_3$, **4c**;
R = Me: L = CH$_3$CN, **4d**

(10) (a) Reference 3a, Chapter 12. (b) Reference 3b, Chapters 4 and 10. For a few examples from Pt(II) and Pd(II) chemistry, see: (c) Whitesides, G. M.; Gaasch, J. F.; Stedronsky, E. R. *J. Am. Chem. Soc.* **1972**, *94*, 5258. (d) Foley, P.; DiCosimo, R.; Whitesides, G. M. *J. Am. Chem. Soc.* **1980**, *102*, 6713. (e) McCarthy, T. J.; Nuzzo, R. G.; Whitesides, G. M. *J. Am. Chem. Soc.* **1981**, *103*, 3396. (f) DiCosimo, R. D.; Moore, S. S.; Sowinski, A. F.; Whitesides, G. M. *J. Am. Chem. Soc.* **1982**, *104*, 124. (g) Reamey, R. H.; Whitesides, G. M. *J. Am. Chem. Soc.* **1984**, *106*, 81. (h) Brainard, R. L.; Whitesides, G. M. *Organometallics* **1985**, *4*, 1550. (i) Moravskiy, A.; Stille, J. K. *J. Am. Chem. Soc.* **1981**, *103*, 4182. (j) Loar, M. K.; Stille, J. K. *J. Am. Chem. Soc.* **1981**, *103*, 4174. (k) Gillie, A.; Stille, J. K. *J. Am. Chem. Soc.* **1980**, *102*, 4933. (l) Komiya, S.; Morimoto, Y.; Yamamoto, A.; Yamamoto, T. *Organometallics* **1982**, *1*, 1528. (m) Nakazawa, H.; Ozawa, F.; Yamamoto, A. *Organometallics* **1983**, *2*, 241. (n) Komiya, S.; Shibue, A. *Organometallics* **1985**, *4*, 687. (o) Komiya, S.; Akai, Y.; Tanaka, K.; Yamamoto, T.; Yamamoto, A. *Organometallics* **1985**, *4*, 1130. (p) Scott, J. D.; Puddephatt, R. J. *Organometallics* **1983**, *2*, 1643. For theoretical studies, see: (q) Tatsumi, K.; Hoffman, R.; Yamamoto, A.; Stille, J. K. *Bull. Chem. Soc. Jpn.* **1981**, *54*, 1857. (r) Komiya, S.; Albright, T. A.; Hoffman, R.; Kochi, J. K. *J. Am. Chem. Soc.* **1977**, *99*, 8440.

(11) Nyholm, R. S. *Proc. Chem. Soc.* **1961**, 273.

(12) Atwood, J. D. *Inorganic and Organometallic Reaction Mechanisms*; Brooks/Cole: Monterey, CA, 1985; Chapter 2.

(13) Garrou, P. E.; Heck, R. F. *J. Am. Chem. Soc.* **1976**, *98*, 4115.

(14) Both the insertion and the deinsertion (reverse) steps in eq 1 are also promoted by the presence of electron-donating substituents on R, see: (a) Reference 13. (b) Kubota, M.; Blake, D. M.; Smith, S. A. *Inorg. Chem.* **1971**, *10*, 1430. (c) Cawse, J. N.; Fiato, R. A.; Pruett, R. L. *J. Organomet. Chem.* **1979**, *172*, 405.

Scheme II

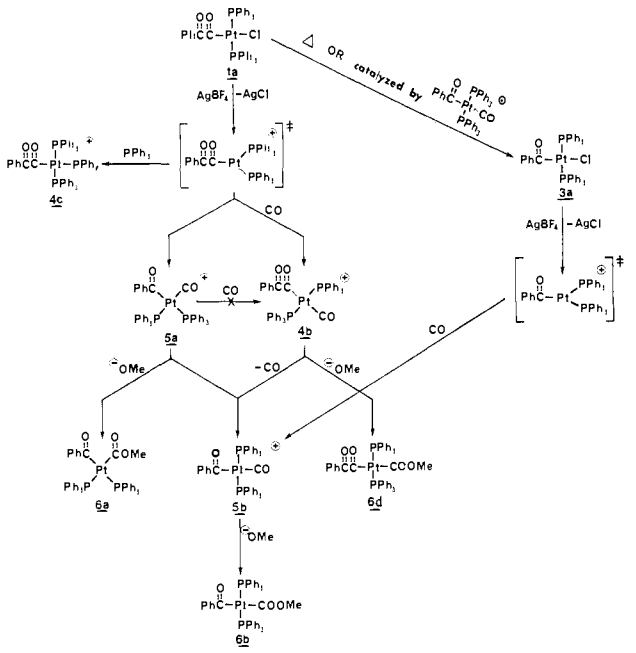

In the absence of any externally added ligands, however, **1a** was found to undergo rapid deinsertion of CO following Cl^- abstraction. At 20 °C in $CHCl_3$, the initial product formed was *cis*-$Pt(PPh_3)_2(CO)(COPh)^+BF_4^-$ (**5a**), an expected derivative arising through a cis migration of the acyl group. The ^{31}P NMR spectrum of **5a** consisted of two doublets accompanied by ^{195}Pt satellites, due to the inequivalence of the two PPh_3 groups. The structure of this complex was further confirmed by its reaction with NaOMe to yield *cis*-$Pt(PPh_3)_2(COMe)(COPh)$ (**6e**) (see section D).

The compound **5a** was stable indefinitely in $CHCl_3$ solution at −40 °C; however, at 25 C, it was observed to slowly isomerize to the corresponding trans compound, *trans*-$Pt(PPh_3)_2(CO)(COPh)^+BF_4^-$ (**5b**). This latter compound exhibited a singlet along with the corresponding ^{195}Pt satellites in the ^{31}P NMR spectrum. In addition, the IR spectrum contained a sharp absorbance at 2070 cm^{-1} due to the terminal CO and a broad band at 1625 cm^{-1}, ascribable to the carbonyl group of the acyl ligand. The structure of this complex was further confirmed by its reaction with NaOMe to yield *trans*-$Pt(PPh_3)_2(COMe)(COPh)$ (**6b**) (see section D). Finally, **5b** was synthesized independently by Cl^- abstraction from the known compound, *trans*-$Pt(PPh_3)_2(Cl)(COPh)$ (**3a**), in $CHCl_3$ that was presaturated with CO.

The cis–trans isomerization reaction, **5a** → **5b**, was examined briefly and was found to be first order in the metal complex. In addition, bubbling CO through the reaction solution was found to significantly accelerate the isomerization process. We note that ligand-assisted cis–trans isomerization of d^8 square-planar complexes is well precedented.[15] The various transformations described above are summarized in Scheme II. An analogous chemistry leading to the formation of *cis*- and *trans*-$Pt(PPh_3)_2(CO)(COMe)^+BF_4^-$ was observed following Cl^- abstraction from **1e** in $CHCl_3$.

Although the neutral compound, **1a**, showed no tendency to deinsert CO in solution below 65 °C, its conversion to the corresponding benzoyl compound, **3a**, could be catalyzed by the cationic compound, **5b**. For example, the addition of 20% **5b** to a $CHCl_3$ solution of **1a** at 20 °C resulted in the quantitative conversion of the latter to **3a** in 2 days. There was little change (<10%) in the concentration of **5b** in the course of this reaction. A plausible mechanism for this catalytic reaction is shown in eq 13 and involves Cl^- abstraction from **1a** by **5b**, followed by rapid CO deinsertion from the newly formed cationic complex. Since **5b** was generated from **1a** following Cl^- abstraction by $AgBF_4$, it was only necessary to add catalytic quantities of $AgBF_4$ to convert **1a** to **3a**.

(15) Anderson, G. K.; Cross, R. *Chem. Soc. Rev.* **1980**, *9*, 185.

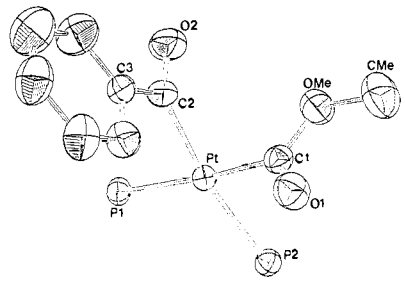

Figure 8. ORTEP drawing of *cis*-$Pt(PPh_3)_2(COPh)(COOMe)$.

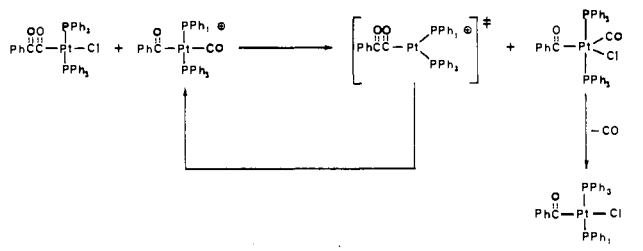

(13)

D. Synthesis and Characterization of the Acyl–Alkoxycarbonyl Complexes. As shown below, the cationic acylcarbonyl complexes, **4b** and **5a**,**b**, have two potential sites that are capable of undergoing nucleophilic attack. Nucleophilic attack along route A would

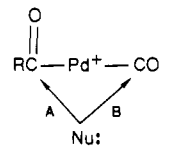

lead to the formation of RCONu and constitutes a possible mechanism for the formation of such species (where Nu = OH, OR, NR_2) from metal-acyl compounds and the corresponding nucleophiles.[16] On the other hand, attack by nucleophiles along path B[17,18] would result in the formation of RCO–Pd–CONu species,[18] which are postulated intermediates in the Pd(II)-catalyzed double carbonylation of alkyl and aryl halides (Scheme I).[5,8] Thus, it was of some interest to find out the preferred pathway for nucleophilic attack on cationic acylcarbonyl complexes.

The compound **5a** was stable for an appreciable length of time only at low temperatures (see section C). Therefore, a CH_2Cl_2 solution of **5a** was prepared in situ at −20 °C by Cl^- abstraction from **1a**, and to this solution was added 1 equiv of NaOMe to form the compound *cis*-$Pt(PPh_3)_2(COPh)(COOMe)$ (**6a**) exclusively. The structure of **6a** was established by ^{31}P NMR and IR spectrscopies and confirmed by X-ray crystallography. The ^{31}P NMR spectrum consisted of two doublets, accompanied by ^{195}Pt satellites, due to the inequivalence of the two PPh_3 groups. The chemical shift and the J_{Pt-P} value for one of the phosphines were very similar to those observed for one phosphine in **5a** (Table I) and were assigned to the PPh_3 ligand trans to the COPh group. The IR spectrum exhibited two $\bar{\nu}$(CO) bands at 1632 and 1615 cm^{-1}. The band at higher frequency was assigned to the COOMe group on the basis of the inductive effect of the MeO group and the conjugation of the Ph group. Such an assignment was also

(16) (a) For specific examples, see: Colquhoun, H. M.; Holton, J.; Thompson, D. J.; Twigg, M. V. *New Pathways for Organic Synthesis*; Plenum: New York, 1984; Chapter 6. (b) An alternative mechanism for the formation of RCONu from RCO–M and a nucleophile has been proposed, see ref 8c.

(17) Nucleophilic attack on CO coordinated to transition metals: (a) Reference 3b, Chapter 5. (b) For specific examples involving alkoxides as nucleophiles, see: Angelici, R. J. *Acc. Chem. Res.* **1972**, *5*, 335.

(18) For examples of $M(COOR)_2$ species formed by the attack of alkoxides on coordinated CO, see: (a) Rivetti, F.; Romano, U. *J. Organomet. Chem.* **1978**, *154*, 323. (b) Burk, P. L.; Van Engen, D.; Campo, K. S. *Organometallics* **1984**, *3*, 493. (c) Bryndza, H. E.; Kertchmar, S. A.; Tulip, T. H. *J. Chem. Soc., Chem. Commun.* **1985**, 977.

Table V. Selected Bond Distances (Å) and Angles (Deg) for *cis*-Pt(PPh$_3$)$_2$(COPh)(COOMe)[a]

atom 1	atom 2	distance
Pt	P1	2.313 (1)
Pt	P2	2.359 (1)
Pt	C1	2.031 (4)
Pt	C2	2.047 (4)
OMe	CMe	1.473 (6)
OMe	C1	1.359 (5)
O1	C1	1.211 (5)
O2	C2	1.206 (5)
C2	C3	1.500 (6)

atom 1	atom 2	atom 3	angle
P1	Pt	P2	97.92 (4)
P1	Pt	C1	174.7 (1)
P1	Pt	C2	88.9 (1)
P2	Pt	C1	87.3 (1)
P2	Pt	C2	169.9 (1)
C1	Pt	C2	86.1 (2)
CMe	OMe	C1	116.7 (4)
Pt	C1	OMe	113.7 (3)
Pt	C1	O1	127.0 (4)
OMe	C1	O1	119.3 (4)
Pt	C2	O2	119.3 (4)
Pt	C2	C3	122.2 (3)
O2	C2	C3	118.5 (4)

[a] Numbers in parentheses are estimated standard deviations in the least significant digits.

consistent with the reported data on other alkoxycarbonyl complexes of Pt(II).[17b]

The solid-state structure of **6a** as determined by X-ray crystallography is shown in Figure 8. The four ligands were found to be disposed about the central Pt atom in a square-planar geometry with the two phosphines in mutually cis positions. The Pt–P distance for the PPh_3 group trans to COPh was slightly longer that of the group trans to COOMe (2.359 (1) vs. 2.313 (1) Å; Table V) and was consistent with the smaller J_{Pt-P} value for the former phosphine ligand. The COPh and COOMe ligands were found to lie in the planes perpendicular to the plane of the molecule with the carbonyl vectors pointing in opposite directions.

The trans isomer, *trans*-Pt(PPh$_3$)$_2$(COPh)(COOMe) (**6b**), was prepared by the reaction of 1 equiv of NaOMe with the corresponding trans cationic carbonyl complex, **5b**. The latter was generated in situ in CH_2Cl_2 by Cl^- abstraction from **1a** at 25 °C. The ^{31}P NMR spectrum of **6b** consisted of a singlet with accompanying ^{195}Pt satellites and was consistent with a trans structure with two equivalent PPh_3 ligands. The IR spectrum exhibited two $\bar{\nu}$(CO) bands at 1625 and 1602 cm^{-1} corresponding to the COOMe and COPh groups, respectively. We note that both the bands were at lower wavenumbers than the corresponding bands of the cis compound, **6a**. An analogous reaction of **5b** with 1 equiv of NaOEt resulted in the formation of *trans*-Pt(PPh$_3$)$_2$(COPh)(COOEt) (**6c**).

The compound, *trans*-Pt(PPh$_3$)$_2$(COCOPh)(COOMe) (**6d**), was synthesized by the reaction of 1 equiv of NaOMe with the corresponding cationic species, **4b**. The latter was generated in situ in CH_2Cl_2 by Cl^- abstraction from **1a** in the presence of CO (see eq 12). **6d** was purple in sharp contrast to **6a–c** which were yellow. The ^{31}P NMR spectrum of **6d** consisted of a singlet along with the ^{195}Pt satellites and was consistent with the proposed trans structure. The IR spectrum exhibited three $\bar{\nu}$(CO) absorptions at 1662, 1632, and 1628 cm^{-1} that were assigned to the β- and α-carbonyl groups of the PhCOCO ligand and the carbonyl group of the MeOCO ligand, respectively, by comparison with the corresponding $\bar{\nu}$(CO) bands at **1a** and **6b**. The ^{13}C NMR spectrums of **6d** contained three resonances due to the carbonyl carbons at 258.15, 199.77, and 194.24 ppm, respectively. The most downfield resonance exhibited J_{Pt-C} = 9.3 Hz and was assigned to the carbonyl group of the MeOCO ligand. The resonance at 199.77 ppm, showing J_{Pt-C} = 13.9 Hz, was attributed to the α-carbonyl group of the PhCOCO ligand, and the highest field resonance, which showed no discernible ^{195}Pt–^{13}C coupling, was assigned to the β-carbonyl group. The compound **6d** was readily soluble in chlorinated and aromatic solvents but was found to decompose slowly in solution even at 0 °C. A number of decomposition products were observed in the ^{31}P NMR spectrum, one of which was identified as **6b**.

Table VI. Data Relating to X-ray Crystallography

	1a	6a
	A. Crystal Data	
empirical formula	$C_{44}H_{35}ClO_2P_2Pt$	$C_{45}H_{38}O_3P_2Pt$
fw	888.26	883.84
F(000)	3520	1760
cryst dimens, mm	0.13 × 0.58 × 0.59	0.42 × 0.54 × 0.58
Mo Kα radiation: λ, Å	0.71073	0.71073
temp, °C	22 (2)	21 (2)
space group	orthorhomic *Pbca*	monoclinic $P2_1/n$
cell dimens		
a, Å	11.904 (4)	9.885 (3)
b, Å	23.255 (5)	19.812 (3)
c, Å	26.797 (4)	19.557 (2)
β, deg		94.85 (2)
vol, Å^3	7418 (5)	3816 (3)
Z	8	4
density (calcd), g/cm^3	1.591	1.540
abs coeff (μ), cm^{-1}	40.16	38.38
	B. Intensity Measurements	
scan type	ω–2θ	ω–2θ
scan width, deg	1.1 + 0.35 tan θ	1.0 + 0.35 tan θ
max 2θ, deg	41.0	45.4
no. of reflns measd	5572	5603
corrections	Lorentz–polarization	Lorentz–polarization
anisotropic decay	from 0.947 to 1.202 on I	from 0.988 to 1.677 on I
empirical abs		from 0.754 to 1.00 on I
	C. Structure Solution and Refinement	
solution	Patterson method	Patterson method
hydrogen atoms	not included	not included
minimization function	$\sum w(\|F_o\| - \|F_c\|)^2$	$\sum w(\|F_o\| - \|F_c\|)^2$
least-squares weights	$4F_o^2/\sigma^2(F_o^2)$	$4F_o^2/\sigma^2(F_o^2)$
no. of reflns included	2973 with $I > 3\sigma(I)$	4393 with $I > 3\sigma(I)$
data: parameter ratio	6.8	15.69
unweighted agreement factor	0.082	0.043
weighted agreement factor	0.097	0.056
esd in observn of unit weight	3.709	3.499
convergence, largest shift	0.07σ	0.01σ
final p parameters in weighing scheme	0.035	0.020

Experimental Section

Analytical Instrumentation. IR spectra were recorded on a Perkin-Elmer Model 281B spectrometer. ^1H and ^{13}C NMR spectra were recorded on a Bruker WP200 FT-NMR spectrometer. ^{31}P NMR spectra were recorded on a Varian CFT-20 spectrometer. UV–vis spectra were recorded on a Hewlett-Packard Model 8450A or a Varian Model Cary 118 spectrometer. X-ray diffraction data were obtained by using an Enraf-Nonius CAD4 diffractometer with a graphite crystal, incident beam, and monochromator; structure solution and refinement were carried out on a PDP-11/34a or a VAX-11/750 computer using the SDP-PLUS software (Enraf-Nonius & B. A. Frenz Assoc.). Elemental analysis was performed by Galbraith Laboratories, Knoxville, TN.

General Procedure. Reagent grade chemicals were used. The solvents were dried by distillation from CaH_2. All solvents and liquid chemicals were deoxygenated either by vacuum distilling or by purging with N_2 prior to use. The metal compounds were stored in a N_2 filled drybox.

M(PPh$_3$)$_4$ (M = Pt,[19] Pd[20]) were prepared by literature methods. The α-ketoacyl chlorides were synthesized from the corresponding α-keto acids by the reaction with α,α-dichloromethyl methyl ether.[21] Benzo-

(19) Ugo, R.; Cariati, F.; La Moncia, G. *Inorg. Synth.* **1968**, *11*, 105.
(20) Coulson, D. R. *Inorg. Synth.* **1970**, *13*, 121.

Table VII. Positional Parameters and Their Estimated Standard Deviations for *trans*-$Pt(PPh_3)_2(Cl)(COCOPh)$[a]

atom	x	y	z	B, Å²
Pt	0.10703 (7)	0.17406 (4)	0.13603 (3)	3.49 (2)
Cl	0.0840 (6)	0.1668 (3)	0.0465 (2)	5.9 (2)
P1	0.0747 (5)	0.2718 (2)	0.1332 (2)	3.6 (1)
P2	0.1390 (4)	0.0762 (2)	0.1373 (2)	3.4 (1)
O1	0.241 (1)	0.2057 (1)	0.2220 (6)	5.9 (4)
O2	−0.020 (1)	0.1428 (7)	0.2312 (6)	6.0 (4)
C1	0.146	0.182	0.209	4.4 (8)*
C1A	0.059	0.166	0.209	3 (1)*
C2	0.059	0.166	0.250	4.5 (7)*
C2A	0.147	0.195	0.250	9 (2)*
C3	0.135 (3)	0.180 (1)	0.3045 (9)	16 (1)
C4	0.211 (2)	0.1745 (9)	0.324 (1)	6.0 (6)
C5	0.214 (2)	0.1815 (9)	0.3787 (9)	6.3 (7)
C6	0.135 (3)	0.187 (1)	0.406 (1)	11 (1)
C7	0.013 (3)	0.182 (1)	0.379 (1)	9 (1)
C8	0.007 (2)	0.176 (1)	0.330 (1)	8.4 (9)
C10	0.083 (2)	0.307 (1)	0.1937 (8)	4.4 (6)
C11	0.163 (2)	0.347 (1)	0.205 (1)	7.5 (8)
C12	0.161 (3)	0.374 (1)	0.253 (1)	11 (1)
C13	0.075 (3)	0.360 (1)	0.289 (1)	9.3 (9)
C14	−0.007 (3)	0.319 (1)	0.2752 (9)	8.7 (8)
C15	−0.006 (2)	0.293 (1)	0.2277 (8)	4.9 (6)
C20	0.183 (2)	0.3039 (9)	0.0946 (9)	5.0 (6)
C21	0.150 (2)	0.345 (1)	0.058 (1)	6.7 (7)
C22	0.239 (3)	0.368 (1)	0.029 (1)	9.0 (9)
C23	0.345 (2)	0.352 (1)	0.037 (1)	8.8 (8)
C24	0.374 (3)	0.308 (1)	0.071 (1)	10 (1)
C25	0.294 (2)	0.284 (1)	0.102 (1)	8.4 (9)
C30	−0.058 (2)	0.2980 (9)	0.1065 (8)	3.9 (5)
C31	−0.115 (2)	0.3425 (9)	0.1281 (8)	5.4 (6)
C32	−0.214 (2)	0.364 (1)	0.1051 (9)	5.5 (7)
C33	−0.252 (2)	0.338 (1)	0.0610 (9)	7.2 (8)
C34	−0.192 (2)	0.295 (1)	0.038 (1)	6.5 (7)
C35	−0.095 (2)	0.273 (1)	0.0596 (9)	5.6 (6)
C40	0.271 (2)	0.052 (1)	0.1074 (8)	4.4 (5)
C41	0.325 (2)	0.000 (1)	0.1253 (9)	5.7 (7)
C42	0.425 (2)	−0.016 (1)	0.101 (1)	5.8 (7)
C43	0.472 (2)	0.014 (1)	0.067 (1)	7.4 (7)
C44	0.424 (2)	0.065 (1)	0.047 (1)	7.8 (8)
C45	0.317 (2)	0.085 (1)	0.0688 (9)	4.8 (6)
C50	0.146 (2)	0.0432 (8)	0.1985 (9)	4.2 (5)
C511	0.242 (2)	0.059 (1)	0.2295 (8)	4.8 (6)
C52	0.246 (2)	0.038 (1)	0.2793 (8)	5.9 (7)
C53	0.157 (2)	0.001 (1)	0.2968 (9)	5.9 (7)
C54	0.070 (2)	−0.011 (1)	0.2667 (8)	6.5 (7)
C55	0.066 (2)	0.009 (1)	0.2170 (9)	5.2 (6)
C60	0.029 (2)	0.0411 (8)	0.1064 (7)	3.3 (5)
C61	0.040 (2)	−0.010 (1)	0.0774 (9)	5.6 (7)
C62	−0.054 (2)	−0.035 (1)	0.053 (1)	7.5 (8)
C63	−0.159 (2)	−0.011 (1)	0.0582 (9)	5.2 (6)
C64	−0.175 (2)	0.0398 (9)	0.0864 (8)	4.9 (6)
C65	−0.080 (2)	0.064 (1)	0.1111 (8)	4.8 (6)

[a] Asterisks indicate that the atoms were found to be disordered and were not allowed to refine. Anisotropically refined atoms are given in the form of the isotropic equivalent parameter defined as $^4/_3[a^2\beta_{11} + b^2\beta_{22} + c^2\beta_{33} + ab(\cos\gamma)\beta_{12} + ac(\cos\beta)\beta_{13} + bc(\cos\alpha)\beta_{23}]$. Numbers in parentheses are estimated standard deviations.

Table VIII. Positional Parameters and Their Estimated Standard Deviations for *cis*-$Pt(PPh_3)_2(COPh)(COOMe)$[a]

atom	x	y	z	B, Å²
Pt	0.48792 (3)	0.18166 (1)	0.26593 (1)	2.107 (6)
P1	0.4902 (2)	0.1183 (1)	0.3653 (1)	2.55 (4)
P2	0.6096 (2)	0.1060 (1)	0.2010 (1)	2.43 (4)
OMe	0.3573 (6)	0.2435 (3)	0.1456 (3)	4.3 (1)
O1	0.5695 (6)	0.2795 (3)	0.1654 (3)	4.3 (1)
O2	0.2396 (6)	0.2348 (4)	0.3057 (3)	5.0 (2)
OMe	0.350 (1)	0.2791 (6)	0.0793 (6)	5.9 (3)
C1	0.4790 (7)	0.2444 (4)	0.1835 (4)	2.7 (2)
C2	0.3588 (7)	0.2482 (4)	0.3071 (4)	2.9 (2)
C3	0.4077 (8)	0.3128 (4)	0.3407 (4)	2.9 (2)
C4	0.5337 (9)	0.3388 (5)	0.3314 (5)	3.9 (2)
C5	0.580 (1)	0.3984 (5)	0.3642 (5)	5.0 (2)
C6	0.497 (1)	0.4311 (5)	0.4089 (5)	5.2 (3)
C7	0.374 (1)	0.4038 (5)	0.4189 (6)	6.1 (3)
C8	0.326 (1)	0.3465 (5)	0.3841 (6)	5.1 (2)
C11	0.4166 (8)	0.1560 (4)	0.4386 (4)	3.0 (2)*
C12	0.295 (1)	0.1355 (6)	0.4607 (6)	5.2 (2)*
C13	0.246 (1)	0.1691 (6)	0.5201 (7)	6.8 (3)*
C14	0.319 (1)	0.2196 (6)	0.5521 (6)	5.9 (3)*
C15	0.440 (1)	0.2401 (6)	0.5298 (6)	5.6 (2)*
C16	0.487 (1)	0.2094 (5)	0.4714 (5)	4.4 (2)*
C21	0.3943 (8)	0.0405 (4)	0.3478 (4)	3.0 (2)*
C22	0.2686 (9)	0.0497 (5)	0.3120 (5)	4.2 (2)*
C23	0.186 (1)	−0.0076 (6)	0.2944 (6)	6.0 (3)*
C24	0.232 (1)	−0.0709 (6)	0.3109 (6)	5.8 (3)*
C25	0.360 (1)	−0.0806 (5)	0.3465 (6)	5.2 (2)*
C26	0.4410 (9)	−0.0243 (5)	0.3652 (5)	3.9 (2)*
C31	0.6578 (8)	0.0986 (4)	0.4053 (4)	2.8 (2)*
C32	0.7670 (9)	0.1306 (5)	0.3817 (5)	3.6 (2)*
C33	0.900 (1)	0.1209 (5)	0.4144 (5)	4.9 (2)*
C34	0.917 (1)	0.0789 (5)	0.4710 (6)	5.1 (2)*
C35	0.807 (1)	0.0471 (5)	0.4962 (5)	5.0 (2)*
C36	0.6756 (9)	0.0579 (5)	0.4644 (5)	4.0 (2)*
C41	0.5254 (7)	0.1014 (4)	0.1149 (4)	2.6 (1)*
C42	0.595 (1)	0.1106 (5)	0.0570 (5)	4.7 (2)*
C43	0.524 (1)	0.1071 (7)	−0.0080 (7)	7.2 (3)*
C44	0.384 (1)	0.0935 (7)	−0.0157 (7)	7.7 (3)*
C45	0.315 (1)	0.0866 (6)	0.0435 (6)	5.7 (2)*
C46	0.3878 (9)	0.0898 (5)	0.1086 (5)	3.8 (2)*
C51	0.7848 (7)	0.1301 (4)	0.1907 (4)	2.5 (1)*
C52	0.8336 (8)	0.1907 (4)	0.2187 (4)	2.8 (2)*
C53	0.9700 (9)	0.2076 (5)	0.2163 (5)	3.4 (2)*
C54	1.0586 (9)	0.1643 (5)	0.1851 (5)	3.8 (2)*
C55	1.0080 (9)	0.1049 (5)	0.1569 (5)	3.9 (2)*
C56	0.8720 (8)	0.0865 (4)	0.1599 (5)	3.6 (2)*
C61	0.6326 (7)	0.1069 (4)	0.2257 (4)	2.6 (1)*
C62	0.5401 (9)	−0.0332 (5)	0.1987 (5)	4.2 (2)*
C63	0.564 (1)	−0.1004 (5)	0.2204 (5)	4.6 (2)*
C64	0.671 (1)	−0.1171 (5)	0.2664 (5)	4.8 (2)*
C65	0.761 (1)	−0.0690 (5)	0.2934 (5)	4.5 (2)*
C66	0.7402 (9)	−0.0002 (4)	0.2723 (4)	3.5 (2)*

[a] Asterisks indicate that the atoms were refined isotropically. Anisotropically refined atoms are given in the form of the isotropic equivalent parameter defined as $^4/_3[a^2\beta_{11} + b^2\beta_{22} + c^2\beta_{33} + ab(\cos\gamma)\beta_{12} + ac(\cos\beta)\beta_{13} + bc(\cos\alpha)\beta_{23}]$. Numbers in parentheses are estimated standard deviations.

ylformic acid and pyruvic acid were obtained commercially. The other α-keto acids were prepared by literature methods.[22]

Synthesis of *trans*-$M(PPh_3)_2(Cl)(COCOR)$ (1a–e, 2). The α-ketoacyl chloro complexes were synthesized by the oxidative addition reaction of the corresponding α-ketoacyl chlorides with $M(PPh_3)_4$. Because of the air-sensitivity of $M(PPh_3)_4$, all the reactions were carried out under an N_2 atmosphere. In a typical reaction, 1.5 g of $Pt(PPh_3)_4$ was dissolved in 50 mL of C_6H_6, and to this solution was added 0.2 mL of PhCOCOCl with stirring at 25 °C. After further stirring for 2 h, the resulting red-orange solution was filtered. The filtrate on evaporation of the solvent gave a red, oily residue. This was washed with Et_2O and recrystallized from a CH_2Cl_2/Et_2O mixture to give an orange crystalline product: yield 1.0 g (75%); UV–vis λ_{max} (toluene) 484 nm (ϵ_{max} 67.2).

Anal. Calcd for $C_{44}H_{35}O_2P_2ClPt$: C, 59.46; H, 3.94. Found: C, 59.91; H, 4.24. The compounds **1b–e** were prepared analogously and characterized by elemental analysis and ^{31}P NMR, ^1H NMR, and IR spectroscopies.

In the synthesis of **2**, 1.5 equiv of PPh_3 was added to $Pd(PPh_3)_4$ before the addition of PhCOCOCl, and the reaction was carried out at 0 °C. These modifications were made to retard the decomposition of **2** in solution. Following workup and recrystallization, a salmon-pink crystalline product was obtained: yield 86%; UV–vis λ_{max} (CH_2Cl_2) 494 nm (ϵ_{max} 80). Anal. Calcd for $C_{44}H_{35}O_2P_2ClPd$: C, 66.04; H, 4.38; P, 7.75. Found: C, 66.22; H, 4.50; P, 7.58.

Synthesis of *trans*-$Pt(PPh_3)_2(L)(COCOR)^+BF_4^-$ (4a–d). The cationic α-ketoacyl compounds were synthesized by Cl^- abstraction from the corresponding neutral compounds in the presence an added ligand, L. In a typical reaction, 40 mL of CH_3CN was added with stirring to a mixture consisting of 0.34 g of **1a** and 0.08 g of $AgBF_4$. A yellow solution together with a white precipitate of AgCl was formed. CH_3CN was removed from this reaction mixture, and the residue was extracted with CH_2Cl_2. **4a**, in the form of a light-yellow solid, was obtained following

(21) (a) Ottenheim, H. C. J.; DeMar, J. H. M. *Synthesis* **1975**, 163. (b) Ottenheim, H. C. J.; Tijhuis, M. W. *Org. Synth.* **1983**, 61, 1.
(22) Nimitz, J. S.; Mosher, H. S. *J. Org. Chem.* **1981**, *46*, 211.

the evaporation of CH_2Cl_2 from the extract, yield 0.34 g (90%). The compound **4d** was prepared analogously: ^1H NMR ($CDCl_3$) (ppm) **4a** 1.50 (3 H, CH_3CN), **4d** 1.52 (3 H, CH_3CN), 0.92 (3 H, $COCOCH_3$).

1a (0.1 g) was used for the preparation of compounds **4b** and **4c**, and the Cl^- abstraction was carried out in CH_2Cl_2 or $CHCl_3$ in the presence of excess PPh_3 (1.5 g) and CO (saturated), respectively. The compounds were characterized by ^{31}P NMR spectroscopy.

Synthesis of *cis*- and *trans*-Pt(PPh_3)$_2$(CO)(COPh)$^+BF_4^-$ (5a–b). The cationic cis complex, **5a**, was prepared in situ in $CHCl_3$ by the addition of 1 equiv of $AgBF_4$ to 0.5 g of **1a** at −40 °C. The trans isomer, **5b**, was synthesized analogously at 25 °C. Following filtration to remove precipitated AgCl, the solvent was evaporated from the filtrate to yield solid **5b**. Alternatively, in a procedure analogous to that used to make **4b**, **5b** was made by Cl^- abstraction from *trans*-Pt(PPh_3)$_2$(Cl)(COPh) in $CHCl_3$ in the presence of CO: yield 80%. Anal. Calcd for $C_{44}H_{35}O_2P_2BF_4Pt$: C, 56.26; H, 3.73. Found: C, 56.56; H, 4.00.

Synthesis of *cis*- and *trans*-Pt(PPh_3)$_2$(COPh)(COOR) (6a–c). The acyl–alkoxycarbonyl complexes were prepared by the reaction of the corresponding cationic acyl–carbonyl compounds with alkoxides. In a typical reaction, a solution of **5a** in CH_2Cl_2 was generated at −20 °C by the addition of 1 equiv of $AgBF_4$ to 0.5 g of **1a**. This solution was filtered at −20 °C to remove precipitated AgCl. To the filtrate, 1 equiv of NaOMe was added with stirring at −20 °C, resulting in the formation of **6a** and the precipitation of $NaBF_4$. After the reaction mixture was allowed to warm up to 25 °C, it was filtered, and **6a** was isolated from the filtrate by removal of the solvent. Following recrystallization from CH_2Cl_2–petroleum ether, a yellow crystalline solid was obtained: yield 55%; ^1H NMR ($CDCl_3$) (ppm) 2.80 (3 H, $COOCH_3$). Anal. Calcd for $C_{45}H_{38}O_3P_2Pt$: C, 61.15; H, 4.30. Found: C, 60.10; H, 4.47. The compounds **6b** and **6c** were made analogously by the reaction of the CH_2Cl_2 solution of **5b** with the corresponding alkoxides. **6b**: yield 67%. ^1H NMR ($CDCl_3$) (ppm) 2.48 (3 H, $COOCH_3$). Anal. Calcd for $C_{45}H_{38}O_3P_2Pt$: C, 61.15; H, 4.30. Found: C, 60.35; H, 4.62.

Synthesis of *trans*-Pt(PPh_3)$_2$(COCOPh)(COOMe) (6d). This compound was prepared by a procedure analogous to that used to make **6a–c**. The addition of 1 equiv of NaOMe to a CH_2Cl_2 solution containing 0.5 g of **4b** at 25 °C resulted in the formation of a purple solution. This reaction mixture was filtered, and solid **6d** was obtained from the filtrate by evaporation of the solvent. Recrystallization from CH_2Cl_2–Et_2O yielded a purple crystalline solid: yield 63%; Anal. Calcd for $C_{46}H_{38}O_4P_2Pt$: C, 60.57; H, 4.17. Found: C, 60.02; H, 4.70. ^1H NMR ($CDCl_3$) (ppm) 2.37 (3 H, $COOCH_3$) ; $^{13}C\{^1H\}$ NMR ($CDCl_3$) (ppm) 258.15 ($J_{C\text{-}P}$ = 9.3 Hz, *C*OOCH$_3$), 199.77 ($J_{C\text{-}P}$ = 13.9 Hz, *C*OCOPh), 194.24 (CO*C*OPh), 48.00 (COO*C*H$_3$); UV–vis λ_{max} (CH_2Cl_2) 504 nm.

Kinetics. The conventional spectrophotometric method was employed for kinetic measurements. The α-ketoacyl chloro complex was the limiting reagent in all runs. The disappearance of the starting complex was followed by monitoring the decrease in intensity of the absorption maximum which was at 494, 484, 482, 488, and 480 nm for **2** and **1a–d**, respectively. For the decomposition of **2**, the concentration of the complex was approximately 6.7×10^{-3} M and the concentration of added PPh_3 was varied between 3×10^{-3} and 7×10^{-2} M. For the decomposition of **1a–d**, the concentration of the complex was 2.3×10^{-3} M and the concentration of the added PPh_3 was 8.99×10^{-2} M. In all cases, the plot of ln ($A_t - A_\infty$) vs. time was linear for at least three half-lives. A nonlinear least-squares program was applied on all the kinetic data, and correlation values between 0.995 and 1.000 were considered to be satisfactory.

Studies under High CO Pressures. (a) Five milliliters of a CH_2Cl_2 solution that was 5.0×10^{-3} M in **2** and 6.67×10^{-2} M in PPh_3 was split into two portions and placed in two optical cells. One cell was placed in a bomb that was subsequently pressured up to 700 psi with CO. The second cell was left under 1 atm of N_2. At intervals, the first cell was taken out of the bomb and its solution absorbance compared with that of the second sample.

(b) A solution containing 0.110 g of **3b** and 0.017 g of PPh_3 in 2.6 mL of CH_2Cl_2 was placed in a bomb that was then pressured up to 1000 psi with CO. After 30 min, the bomb was opened and the solution absorbance measured immediately (dead time interval < 15 s). An absorbance change of <0.01 at 494 nm was obtained. The solubility of CO in $CHCl_3$ at 25 °C and 15 psi of pressure is 0.19 mL/mL of $CHCl_3$[23] (i.e., 8.5×10^{-3} M). By use of Henry's law, the concentration of CO at 1000 psi would be 0.56 M. Assuming the solubility of CO in CH_2Cl_2 to be similar to that in $CHCl_3$,[24] K_{eq} for **2** ⇌ **3b** + CO may be estimated by eq 14.

$$K_{eq} = \frac{[3b][CO]}{[2]} > \frac{(0.05\ M)(0.56\ M)}{[0.01/(80\ M^{-1}\ cm^{-1})(1\ cm)]} = 224 \quad (14)$$

X-ray Crystal Structure Determinations. Crystals of **1a** and **6a** were isolated by the slow evaporation of their solutions in C_6H_6–Et_2O and CH_2Cl_2–Et_2O, respectively. Data relating to the determination of their crystal structures are summarized in Table VI. For **1a**, a positional disorder existed for the two carbonyl carbon atoms because of a 180° rotation about the twofold axis through the Pt–Cl bond (Figure 3). In the final least-squares cycle, all non-hydrogen atoms except the two disordered carbon atoms were refined anisotropically, no attempt being made to refine the positional disorder.

Selected bond distances and bond angles for **1a** and **6a** are given in Tables II and V, respectively; the positional parameters are given in Tables VII and VIII, respectively.

Acknowledgment. Support of this research through grants from the U.S. Department of Energy, Office of Basic Energy Sciences (DE-FG02-84ER13295), and the Donors of the Petroleum Research Fund, admininstered by the American Chemical Society, is gratefully acknowledged. We also thank Johnson Matthey, Inc., for generous loans of platinum and palladium salts.

Supplementary Material Available: Tables of bond lengths, bond angles, and thermal parameters for **1a** and **6** (13 pages); tables of calculated and observed structure factors for **1a** and **6a** (74 pages). Ordering information is given on any current masthead page.

(23) *International Critical Tables of Numerical Data, Physics, Chemistry and Technology*; Washburn, E. W., Ed.; McGraw-Hill: New York, 1928; Vol. 3, p 265.

(24) The solubilities of CO in MeOH, Me_2CO, PhH, and $PhCH_3$ differ from that in $CHCl_3$ by less than 15% at 25 °C.[23]